REACTOR CENTRUM NEDERLAND

RCN-41

RCN REPORT

CALCULATION OF THE SAFE LIFE TIME EXPECTANCY OF ZIRCONIUM ALLOY CANNING IN THE FUEL-ELEMENTS OF THE NERO REACTOR

by: A.van der Linde.

Petten, July 1965

REACTOR CENTRUM NEDERLAND

RCN-41

Petten, July 1965.

Subject: Calculation of the safe life time expectancy of Zirconium alloy canning in the fuel-elements of the NERO reactor

By : A. van der Linde

To : Management
Heads of Departments
Author (100x)

Table of contents

Introduction

The activities of RCN at Petten are partly directed to the development of a nuclear propulsion system for a 65000 tons dwt, 22000 shp ship. The technological part of the development programme is carried out under contract between RCN and Euratom. The design target is a pressurized water reactor with internal recirculation, a thermal rating of 61 MW and a core life time of 3.3 years at full power. The fuel rods in this reactor, the NERO reactor, will be of the conventional rod-type: sintered UO_2-pellets enclosed in a 1250 mm long tube with an I.D. of 10.20 mm and a W.T. of 0.85 mm. A considerable part of the fuel rods in the NERO core have to operate at a temperature of 345 °C at the outer surface of the hot places of the canning tubes.

During the preliminary state of design Zircaloy-2, being the best known Zirconium alloy at that moment, was chosen as one of the possible canning materials for the fuel. The deleterious effect of hydrogen, absorbed in the canning during operation under PWR conditions, on the mechanical properties made a safe longterm use of the Zircaloy-2 however doubtful. A calculation, performed in 1963, of the safe life time expectancy of Zircaloy-2 canning tubes in the NERO fuel element, was based on the following assumptions:

1. The time to transition is decreased by a factor four in a reactor.
2. The post-transition oxidation rate is increased by a factor two in a reactor.
3. The percentage of hydrogen absorbed is 50% in the pre-transition region and 100% in the post-transition region.
4. The maximum allowable hydrogen content, in our 0.85 mm thick wall, is 300 ppm more than the hydrogen solubility in Zircaloy-2 at the temperature of the oxide-metal interface.

The calculation led to the pessimistic conclusion that the maximum life time of the fuel rods, having a cladding surface temperature of 345 °C, was 1.3 years.

During the past five years a continually increasing number of corrosion experiments were in progress, investigating the behaviour of Zirconium alloys in water, steam and oxygen. Correct interpretation and correlation of the published results is however impeded by:

a) the disagreement in published oxidation- and hydridation rates obtained by different laboratories, caused mainly by different thermal cycling and oxygen content conditions during the experiments,

b) the wide scatter in the data obtained from different test specimens corroded under similar conditions, apparently caused by slight deviations from specified conditions during degreasing, pickling and conditioning treatments,

c) the absence of a fundamental understanding of the oxidation and hydridation mechanism.

In spite of these interpretation difficulties the experimental results not only justify a rectification of the above mentioned assumptions but also ask for a new approach of the calculation methods.

Apart from the chemical composition and the metallurgical state of the Zirconium alloys the oxidation and hydridation rates are influenced by a number of factors which can be divided in:

A. Physical factors

1) Mechanical attack
2) Thermal cycling
3) Pressure effect
4) Galvanic coupling
5) Heat flux

B. Chemical factors

1) Surface pre-treatment
2) Welding treatment
3) Oxygen content of the corrosive medium
4) Hydrogen content of the corrosive medium
5) pH of the corrosive medium

C. Effects of irradiation

In part A, B and C of this report a literature survey will be given of the experimentally observed effects of the just mentioned factors. After a presentation of the RCN results in part D and a summary of the present state of knowledge regarding the oxidation and hydridation mechanism in part E, a kinetic picture of these mechanisms will be presented in part F.

Finally in part G a calculation of the safe life time expectancy of Zirconium alloy canning in the NERO fuel element will be performed.

A. The influence of physical parameters on oxidation and hydridation rates

1. Effect of mechanical attack

1.1 Coupons of Zircaloy-2 corroded to a weight gain of 30-60 mg/dm^2 in 100 atm. steam at 400 °C were bent around a 4.5 cm diameter cylindrical mandrel and subsequently corroded further in steam. By this bending neither the transition point at 39-40 mg/dm^2 nor the post-transition oxidation rate were affected considerably. (A.1)

1.2 Points of fretting attack of Zircaloy-2 pressure tubes, apparently caused by a combination of relative movement between fuel elements and pressure tubes and of corrosion, increase in number and penetration depth with:

a) increased temperature
b) increased vibration
c) increased clearance between the impacting surfaces.

About 2% of approximately 1600 fretting spots were deeper than 0.250 mm. The maximum penetration depth, 0.650 mm, occured in approximately two months of reactor operating time.

After a 20 day test in 315 °C water, flowrate 45-49 m/sec., penetration depths of 25 and 25-125 microns were observed at clearances of 0.125 and 1.25 mm respectively. The hydride content of the fretted area was increased by a factor 1.5-3. (A.2)

2. Effect of thermal cycling

2.1 Zircaloy-4 coupons conditioned for 21 and 49 days in 400 °C, 105 atm. steam and then corroded in 360 °C, 105 atm. steam showed nearly the same corrosion rates after transfer as coupons corroded continuously in 360 °C, 105 atm. steam. (A.3)

2.2 During the corrosion of a Zircaloy-2 coupon in steam of 1 atm. at 425 °C for 85 days the weight was recorded continuously using a thermobalance. No rate transition at all was observed in the 35-40 mg/dm^2 region where transition normally occurs. At about 60-70 mg/dm^2 weight gain the rate began to accelerate. This result is in agreement with Harwell results.

Cooling of the coupons, in the range 35-45 mg/dm^2, to room temperature overnight and reheating to 425 °C the next morning initiated an increase in corrosion rate with a decreasing rate over the next 7 days following the thermal cycle. (A.4)

3. Effect of pressure

3.1 Zircaloy-2 and Zircaloy-4 specimens were exposed to 400 °C steam at 105, 35 and 3.5 atmosphere pressure. The data obtained after 9 months exposure show that the 3.5 atm. coupons exhibit the lowest weight gains. The hydrogen absorption percentage appears generally unaffected by test pressure. (A.3)

3.2 Zircaloy-2 specimens were exposed to 500 °C steam at 0.02, 1.0 and 35 atm. pressure. Nearly the same oxidation rates were measured as well in the pre- as in the post-transition region.

After a sudden pressure increase or decrease an initial high increase, respectively decrease in oxidation rate was followed by a gradually return to the oxidation rate at which it would have been, had the specimen been oxidised at the new pressure to the same weight gain. (A.5)

4. Effect of galvanic coupling

4.1 Galvanic coupling of Zircaloy-2 and 18/8 stainless steels in 300 °C water had little effect on the oxidation rate of Zircaloy-2. The hydrogen absorption however was decreased markedly by the coupling. In most in-pile and out-of-pile corrosion experiments the Zircaloy-2 parts, fuel rods or coupons, are held in place by stainless steel accessories. An improperly passivated stainless steel surface or one that has been ruptured mechanically may thus produce diminution of hydrogen absorption by the Zircaloy-2 parts without this being reflected in the observed weight gains. (A.6)

5. Effect of heat flux

5.1 The oxidation rate of Zircaloy-2 in 300-360 °C water as a function of heat flux was calculated.

Assuming a 50% hydrogen pickup percentage, the time to reach a hydride level of 500 ppm is reduced by about 5% for a 31.5 W/cm^2 increase in heat flux.

However, no account has been taken of a possible acceleration in oxidation rate and a diminution of hydrogen pickup percentage due to irradiation and oxygen in the water. (A.7)

In the last part of this report a calculation of the influence of heat flux on the safe life time expectancy of Zircaloy-2 canning, operating under PWR conditions will be incorporated.

B. The influence of chemical parameters on oxidation and hydridation rates

1. Effect of surface pre-treatment

Pickled Zircaloy-coupons were rinsed in different solutions in order to reduce residual surface fluoride concentrations. None of the tested solutions, under which a $Al(NO_3)_3$ bath, reduced the effect of fluoride contamination. However, a thermal annealing treatment in vacuum during one hour at 650 °C was very successful. Normally prepared coupons showed weight gains ranging from 21-27 mg/dm^2 after 29 days testing in 360 °C water. Annealed coupons showed a weight gain of 23 mg/dm^2 without any spread in the results. (B.1)

2. Effect of welding

Specimens of Zircaloy-4 and Ni-free Zircaloy-2, converted to large α grained material by electron beam welding and annealing, were corrosion tested in 360 °C water and 400 °C steam. Similar characteristics of the oxidation and hydridation rates are exhibited by the coarse and the fine grained alloys. (B.2)

3. Effect of oxygen content

3.1 Autoclave tests in 360 °C degassed water containing oxygen to an overpressure of 70 atm. of Zircaloy specimens, extending to weight gains of 250 mg/dm^2, reached after 543 days, showed the following results (B.3):

a) the presence of oxygen in the water is relatively innocuous to the Zircaloy oxidation rate although slightly higher weight gains are obtained in the oxygenated environment as compared with standard weight gains in degassed 360 °C water,

b) a marked decrease in hydrogen absorption, per unit oxygen weight gain, in the oxygenated environment over that in degassed water was measured.

In 360 °C degassed water Zircaloy-2, nickel-free Zircaloy-2 and Zircaloy-4 absorbed in the pre-transition region respectively 40, 15 and 25% of the theoretically available hydrogen. In the post-transition region these percentages were 78, 22 and 26%.

In oxygenated water all three alloys absorb approximately 5% of the theoretically available hydrogen after the initial 30 mg/dm^2 weight gain as well in the pre- as in the post-transition region. In table I the oxidation and hydridation data for α-annealed Zircaloy-2 in 360 °C water, degassed + oxygen and refreshed, are presented. It is remarkable that the hydridation rate is, apart from the 0-20 mg/dm^2 region and the transition region, linearly dependent on time in degassed water. In the post-transition region the hydridation rate, 2.75 mg/m^2.day, is by about a factor five larger than in the pre-transition region, 0.55 mg/m^2.day. In oxygenated water these rates are reduced by about a factor ten.

3.2 Zircaloy-2 coupons corroded in steam at 400 °C showed a twofold reduction in hydrogen pickup percentage in going from deoxygenated replenished steam, 0.1 ppm O_2, to replenished steam with 3-4 ppm Oxygen. (B.4)

4. Effect of hydrogen content

4.1 Zircaloy-2, nickel-free Zircaloy-2 and Zircaloy-4 coupons were exposed to 360°C, degassed and degassed hydrogenated water under an 2.1 atmosphere overpressure of hydrogen.
After 107 days exposure the weight gains for the three alloys were respectively 53, 30 and 31 mg/dm^2 for the degassed water and 20, 11 and 24 mg/dm^2 for the hydrogenated water. The cumulative hydrogen pickup percentages after those 107 days were 15, 11 and 9% for the nonhydrogenated and 50, 26 and 8% for the hydrogenated conditions (B.5).

4.2 Coupons of Zircaloy-2 were exposed to 315°C degassed water under static autoclave conditions with no hydrogen addition and with 21 atm. hydrogen overpressure. While the corrosion rate increased only slightly the hydrogen pickup percentage increased from 15 to 72% of the theoretically available hydrogen in the early pre-transition region (B.6).

4.3 Coupons of Zircaloy-2 and nickel-free Zircaloy-2 were exposed to 343°C degassed water under static conditions with no hydrogen addition and with 49 atm. hydrogen overpressure.
The tests were only performed in the pre-transition region, up to 32 mg/dm^2 after 140 days for Zircaloy-2 and 40 mg/dm^2 after 140 days for Ni-free Zircaloy-2.
The presence of hydrogen did not increase the oxidation rate. The percentage of hydrogen pickup increased from 26-29% for the nonhydrogenated water to 43-55% for the hydrogenated water for Zircaloy-2. For Ni-free Zircaloy-2 these figures were respectively 6-13 and 19-27% (B.7).

4.4 Zircaloy-2 and Zircaloy-4 coupons subjected to a two week exposure in 343°C water with 0, 35, 70, 105 and 140 atm. hydrogen overpressure showed that the weight gains, ranging from 14 to 22 mg/dm^2 varied nonsystematically with increasing hydrogen overpressure.
The hydrogen pickup however, was found to be a linear function of hydrogen pressure with Zircaloy-2 showing the greatest sensitivity to hydrogen and Zircaloy-4 being virtually unaffected by its presence (B.8).

4.5 During corrosion testing of Zirconium alloys in degassed water in autoclaves the non-absorbed hydrogen accumulates in the water causing an overpressure of hydrogen. For example during a 28 days exposure of hundred Zircaloy-2 specimens, total surface area 28.1 dm^2, in a 2.35 liter autuclave at 360°C a partial hydrogen pressure of approximately 4.2 atm. is produced if a 40% of theoretical hydrogen pickup is accounted for. To investigate a possible influence of the accumulated hydrogen Zircaloy-2 and nickel-free Zircaloy-2 coupons were tested both in static and in refreshed solutions. The results indicate the general equivalence between refreshed and static water testing on both the corrosion and hydrogen absorption kinetics of Zircaloy. (B.9)

5. Effect of pH

5.1 Corrosion coupons of Zircaloy-2 and Zircaloy-4 were exposed to 332°C water containing ammonia to a pH of 12.2. No change in oxidation rate has been noted uptill a weight gain of 70 mg/dm^2 after 538 days exposure as compared with standard oxidation rates in degassed 332°C water (B.10).

5.2 In the pH range 9.0-10.0, obtained by additions of lithium-hydroxide or ammonia, no effect onthe oxidation and hydridation rate was observed neither in static nor in dynamic water. In more concentrated lithium hydroxide solutions, pH $>$12, an acceleration of as well the oxidation as the hydridation rate was measured (B.11).

5.3 Corrosion coupons of Zircaloy-2 and Zircaloy-4 were exposed in two out-of-pile loops containing pH 10 lithium hydroxide solution and oxygen below 0.05 ppm. One loop was operated with 0.03 cm^{3}H$_2$/kg water, the other with 55 cm^{3}H$_2$/kg water. The flow-rate along the specimens was 30 cm/sec., the temperature 322°C. Although the scatter in the results, presented in table 2, is quite evident, an increase in oxidation and hydridation rate is detectable for the hydrogenated solution as compared with the non-hydrogenated solution. In degassed water, see 4.1 and 4.3, the oxidation rate was decreased or unaltered by hydrogen dissolved in the water. The values in table 2 clearly indicates the sensitvity of β-treated Zircaloy-2 to hydrogen in solution (B.12).

C. The influence of neutron and gamma radiation on oxidation and hydridation rates.

1. In-reactor exposure of Zircaloy-2 in watervapour-hydrogen-helium mixtures increases the oxidation rate in the temperature range 290-400°C (C.1).

2. Samples of Zircaloy-2 exposed in a P.W. loop in ETR, no hydrogen added, oxygen content 0.07-2.0 ppm and pH=10, at a temperature of 283°C showed that irradiation, fast flux $\backsim 5.10^{13}$ n/cm^2.sec., increased the weight gains of the samples about tenfold as compared with samples in a similar out-of-pile loop (C.1).

3. In an in-pile loop containing a steam-water-ammonia mixture Zircaloy-2 was exposed to a fast neutron flux of 2.10^{12} n/cm^2.sec. at 285°C. Here also a considerable increase in oxidation rate was observed (C.2).

4. Zircaloy-2 fuel cladding exposed at 300°C in a BWR showed that the time to transition was shortened and the post-transition oxidation rate was increased compared with out-of-pile autoclave tests (C.3).

5. A Zircaloy-2 process tube, operating for approximately 200 days at 204°C in a flux of 3.9-20 10^{12}n/cm^2.sec. ($>$ 1 MeV) was examined for oxide thickness and hydrogen uptake. The oxidation rate, at weight gains not exceeding 40 mg/dm^2 was increased by a factor 5. Assuming a 30% hydrogen absorption percentage no effect of irradiation on hydridation percentage was measured (C.4).

6. Zircaloy-2 specimens irradiated in a fast flux of 1.0 10^{14}n/cm^2.sec. at 285°C showed that the oxidation rate was increased by a factor 1.0-2.2 while the hydridation percentage was not influenced by the irradiation (C.5).

7. Experiments at Harwell resulted in the following conclusions (C.6):
   a) The rate of oxidation of both Zircaloy-2 and Zr-2.5% Nb in 300°C steam increases in a flux of 3.10^{13} fast neutron/cm^2.sec. and a gamma flux of 5.10^8 r/hr.
   b) Before transition the rate is doubled, after transition the rate is increased by a factor ten at 300°C.
   c) The magnitude of the effect decreases as the temperature is raised and at 400°C it becomes negligible.
   d) No enhancement of oxidation rate was detected at $\phi=10^{11}$ n/cm^2.sec. but at 2.10^{12}n/cm^2.sec. it was almost as large as at 3.10^{13}n/cm^2.sec.
   e) During irradiation in 300°C steam the hydrogen absorption changes in proportion to the change in the oxidation rate.

8. Zircaloy-2 coupons were exposed to pH 10 lithiumhydroxide, replenished water containing 25-30 cm^3 hydrogen/kg H_2O in an autoclave at 300°C both at in-pile - in flux and in-pile - out of flux positions. No enhancement of oxidation and hydridation rate was measured comparing coupons exposed in-flux and out-of-flux (C.7).

9. Under PWR conditions, where reliable experience has been accumulated in general no adverse effects of irradiation on oxidation and hydridation of Zircaloy-2 canning have been noted (C.8).

10. No indication of hydrogen accumulation in the walls of a Zircaloy-2 in-pile loop was observed after an exposure of one year in the KEPR at Hanford (C.9).

11. Zircaloy-2 and Zr-2.5% Nb coupons were irradiated in the X-2 loop in the NRX reactor during 125 days at 250°C. The total thermal fluence was 2.3 10^{20}n/cm^2. The water conditions: pH approximately 10 with LiOH, 15-25 ppm hydrogen, flow rate approximately 2 m/sec. Despite the wide scatter in the obtained data, (hydrogen pick-up in Zircaloy-2 ranged from 400-900 µg/dm^2), the results indicate that in the early pre-transition region: (C.10)

    a) The oxidation rate of Zircaloy-2 is increased by a factor 1.3
    b) The hydridation rate of Zircaloy-2 is decreased slightly
    c) The oxidation rate of Zr-2.5% Nb is not affected
    d) The hydridation rate of Zr-2.5% Nb is increased by a factor of about two.

12. Two fuel rods, canned with Zircaloy-2, from Core 1 of the Shipping-port APS, operating almost continuously at 268°C for approximately 21.000 EFPH, were examined for dimensional and microstructural changes, for fission gas release, oxide film thickness and hydrogen content. The reactor conditions, calculated oxide thickness and hydrogen content increase during the three seeds, and the measured values after the third seed are presented in table 3. The calculated hydrogen concentrations were based on a 34% uptake in the pre-transition region. An oxide thickness of one micron equals a weight gain of 15 mg/dm^2.
    The measured values show unequivocally that the oxide growth on and hydrogen accumulation in the Zircaloy-2 cladding was commensurate with the corrosion time-temperature history of the fuel rods based upon corrosion data obtained in out-of-pile autoclaves.(C.11).

13. Oxide films between 0.2 and 0.7 microns thick, on van Arkel zirconium and Zircaloy-2, were irradiated to pure gamma doses of up to 2.10^9 rads and two oxide films were exposed to 10^{17} nvt of fast neutrons.
    Electrical conductivity and capacitance, 100-20.000 c/s., and optical absorption, 2000-20.000 Å, measurements resulted in the following conclusions (C.12):

    a) The cunductivity, capacitance and optical absorption were not detectably altered, neither by gamma doses of up to 2.10^9rads at 20°C nor by fast neutrons, 10^{17} nvt, at 100°C.
    b) The measurements indicate that less than 10^{19} ion displacements/cc were caused in the films.
    c) Theory indicates that less than 10^{17} ion displacements/cc should occur as a consequence of such a gamma dose.
    d) It is highly unlikely that the gamma irradiation experienced by Zircaloy-2 corrosion films, 0.2-0.7 µ thick, in high temperature water reactors could significantly affect electron or ion transport in them.
    e) If, under such conditions, electron or ion transport controls the corrosion of Zircaloy-2, then the corrosion rate should not be altered by reactor gamma radiation.

D. R.C.N. results

1. In 350°C water and 400°C steam, 100 atm., the weight gain of Zircaloy-2 is about 2 mg/dm^2 higher than that of Zircaloy-4 in the region 10-30 mg/dm^2. Beyond this region these two alloys show nearly equal weight gains.

2. The oxidation rate of Zr-2.5% Nb is by about a factor 1.6 higher than that of Zircaloy-2 in the pre-transition region of the Zircaloy-2 curve. Beyond the Zircaloy-2 transition point preliminary results indicate similar oxidation rates for Zircaloy-2 and Zr-2.5% Nb.

3. The transition point of Zircaloy-2 is reached at weight gains of 40 and 60 mg/dm^2 in respectively oxygen and steam at 500°C and at 1 atm. pressure.

4. In 500°C one atm. steam the hydridation follows, apart from the 0-15 and 60-80 mg/dm^2 weight gain range, a rectilinear rate law.

5. From weight gain curves, obtained in our laboratory in autoclaves with canning tube specimens and sheet coupons, the following empirical relations could be calculated for the oxidation of alpha-annealed Zircaloy-2 in 300-360°C water and 400°C, 100 atmospheric steam:

Pre-transition oxidation : $W_{pre} = k_c t^{1/3} = (27.1 \pm 0.8).10^3 t^{1/3}.\exp.(-\frac{5220}{T})$ (D.1)

Post-transition oxidation : $W_{post} = k_l t = (23.0 \pm 0.7).10^8 t.\exp.(-\frac{14400}{T})$ (D.2)

Time to transition: $t_{tr} = (93.0 \pm 3).10^{-9}.\exp.(+\frac{13.300}{T})$ (D.3)

Weight gain at transition : $W_{tr} = (123 \pm 4).\exp.(-\frac{790}{T})$ (D.4)

W = weight gain in mg/dm^2. 15 mg/dm^2 ≡ 1μ thick oxide layer.
T = temperature in °K.
t = time in days.

During these autoclave experiments the number of thermal cycles from operating conditions to room temperature, for weighing the coupons, and heating up again to operating conditions, was approximately eight for the pre-transition region and one per 15 mg/dm^2 weight gain in the post-transition region.

In the relations D.1, D.2, and D.4 the weight gains due to hydrogen absorption is not incorporated. The hydrogen absorption percentage was 33 ± 3% at the end of the pre-transition region and 75 ± 5% in the weight gain region of 100-600 mg/dm^2.
In table 4 the constants k_c, k_l, t_{tr} and W_{tr} are presented for the temperatures 300, 320, 340, 360, and 400°C.

Although our curves deviate somewhat from curves obtained at different laboratories abroad these deviations are not important in relation to the life time calculations presented in part F of this report.
For example, the 142 mg/dm^2 oxygen and 11 mg/dm^2 hydrogen weight gain after 500 days in degassed 360°C water, see table 1, is calculated at 149 ± 4 and 12 mg/dm^2 weight gain of respectively oxygen and hydrogen with the relations D.1-D.4.

E. Summary of the present state of knowledge regarding the oxidation and hydridation mechanism of Zirconium alloys in high temperature water, steam and oxygen.

The present state of knowledge regarding the oxidation and hydridation mechanism can be summarized in the following conclusions obtained and described recently by three different investigators.

HW-82651, July 1964, D.W. Shannon
p. 5.20-5.24 Zirconium hydriding mechanism

1. The corrosion process is controlled by oxygen diffusion from the environment to the metal.
2. The zirconiumoxide corrosion product can be non-stoichiometric, i.e. $ZrO_{1.9}$ to $ZrO_{2.0}$.
3. The corrosion weight gain kinetics initially follow a cubic rate law shifting more or less to a linear rate at "transition". Under certain conditions the linear portion can initially be a series of respective non-linear segments, i.e. multiple rate transitions.
4. In high pressure systems the corrosion rate is relatively independent of oxygen or water pressure.
5. In low pressure systems the post-transition corrosion rate becomes increasingly dependent on pressure during the oxide growth and can fall appreciable below the limiting high pressure value.
6. In the absence of oxidants hydrogen is rapidly absorbed, but concentrations of oxidant sufficient to maintain the normal oxidation rate results essentially in complete inhibition of gas phase hydriding.
7. However, even with oxidants present, very high hydrogen pressures increase the hydriding rate although to a much lower extent than with oxidants absent.
8. The hydriding pick-up fraction during aqueous corrosion has been observed to be high initially, slow down, and then become more rapid after transition.
9. Traces of oxygen present during aqueous corrosion reduce the amount of hydrogen absorbed during corrosion.

AECL-2085, September 1964. C. Roy
Hydrogen distribution in oxidized Zirconium alloys.

1. Segregated tritium was observed in Zircaloy-2, under certain conditions, at grain, twin and phase boundaries, and at metal zones enriched in oxygen.
2. A constant concentration of tritium throughout the oxide film formed in a T_2O atmosphere, irrespective of orientation, was observed.
3. A much higher uniform concentration of tritium was observed in pre-transition oxide than in the metal substrate.
4. In post-transition oxides tritium segregation was observed.
5. Post-transition oxides were found to offer litter protection against tritium permeation.
6. Low solubility of tritium gas was found in both pre- and post-transition oxides.
7. The distribution of tritium in the metal beneath the oxide was affected by the oxygen concentration.

8. Tritium was rejected from the metal layer adjacent to the oxide-metal interface, which is highly enriched in oxygen, to a metal zone of lower oxygen content containing between 4-8% at. oxygen, equivalent to 8000-16000 ppm oxygen by weight.
9. The oxygen content of the metal beneath the oxide is decreasing according to a diffusion like movement of oxygen to the bulk metal.

AERE-R-4820, December 1964. J.K. Dawson

Areview of the kinetics and mechanism of oxidation and hydriding of zirconium, zircaloy-2 and zirconium-2.5% niobium alloy.

Oxidation mechanism

1. In the weight gain range 0.1-0.3 mg/dm^2 the oxidation follows a rectilinear kinetics, independent of film thickness thus indicating a film thickness growth controlled by an interface reaction.
2. In the weight gain range 0.3-1.2 mg/dm^2 a parabolic rate law is followed, controlled by a uniform diffusion through the oxide layer.
3. In the weight gain range 1.2-3.0 mg/dm^2 a logarithmic rate law is followed.
4. From W $\backsimeq$ 3 mg/dm^2 to the transition point, 35-40 mg/dm^2, a cubic rate law forms a useful approximation of the corrision kinetics.
5. There is no difference between the kinetic behaviour of Zircaloy-2 in steam and oxygen at 400°C.
6. Stress induced increase of the oxidation rate was observed at a weight gain of 20 mg/dm^2.
7. The pre-transition region persists much longer for Zircaloy-2, till 40 mg/dm^2, than for pure zirconium, till 20 mg/dm^2, at 400°C.
8. After transition a cyclic behaviour of the weight gain gradually changes into a rectilinear kinetics.
9. In this post-transition region the number of, metallographically observable, oxide layers corresponds to the number of cycles on the weight gain curve.
10. The exact role of alloying elements in the oxidation kinetics is as yet not clear.
11. Large and widely spread precipitate particles are detrimental for the corrosion rate.
12. The rate of oxidation of cold worked Zr-2.5% Nb alloy in water at temperatures up to 360°C is about a factor of two higher than that of Zircaloy-2 in the pre-transition region. Beyon transition the two alloys behave very similarly.
13. The general features of the oxidation curves of Zr-2.5% Nb are qualitatively similar to those of Zircaloy-2, except that transition to approximately linear kinetics is a much more gradual process for the Zr-Nb alloy.

Hydridation mechanism

1. Up to about 1 mg/dm^2 weight gain of Zircaloy-2 a 100% uptake of the hydrogen evolved by the corrosion reaction is suggested.
2. Between 3 mg/dm^2 and the transition point the hydrogen uptake of Zircaloy-2 increases from 5 to 20% of theoretical.
3. Before transition addition of oxygen to 360°C water has little effect on hydrogen absorption by Zircaloy-2.
4. After transition α-annealed Zircaloy-2 absorbs about 80% of the corrosion hydrogen at 360°C.
5. After transition additions of oxygen reduce the hydrogen absorption in both steam and water.

6. Below 400°C the Zr-2.5% Nb alloy absorbs about 10% of the corrosion hydrogen as well in the pre- as in the post-transition region.
7. Enhanced hydrogen absorption occurs when Zircaloy-2 is exposed to water of 340°C containing substantial amounts of dissolved hydrogen, 9000 cc/kg.
8. Absorption of D from D_2O is at 360°C considerably lower than that of H from H_2O.
9. Exposure of Zircaloy to hydrogen, in the absence of sufficient water vapor to maintain film growth, can give rise to rapid penetration to the metal.
10. Alloying additions which are beneficial in preventing hydrogen absorption in the metal are Nb, V, Si, Sb, Cu and Ti.
11. The higher percentage of hydrogen absorbed in the post-transition region compared with that in the pre-transition region can perhaps be attributed to molecular hydrogen liberated at the base of pores and cracks creating thus a high pressure within the finer pores.

F. Kinetic picture of the Oxidation and Hydridation mechanism

Water, steam or oxygen react with a clean oxide-free Zirconium alloy surface according to the equations:

$$Zr + 2\ H_2O \longrightarrow ZrO_2 + 4\ H \qquad (1a)$$

$$Zr + O_2 \longrightarrow ZrO_2 \qquad (1b)$$

Initially the hydrogen evolved by reaction (1a) is completely absorbed by the metal. Besides forming an oxide layer, part of the oxygen in ZrO_2 is absorbed by the metal. The solubility of oxygen in Zircaloy-2 is $15.7.10^{21}$ atoms O/cm^3 compared with an oxygen concentration in the oxide of 56.10^{21} atoms O/cm^3 and a normal oxygen content of 1000 ppm in the Zircaloy-2 equivalent to $0.24.10^{21}$ atoms O/cm^3. Thus although the diffusion coefficient of oxygen in the Zirconium alloy is very much lower, see table 5, than that of oxygen in the oxide, the large oxygen concentration gradient at the oxide metal interface causes a migration of oxygen ions from the oxide to the metal. This diffusing oxygen is not used for the formation of the oxide layer. The reactions occuring at the oxide-metal interface can be presented by the equations.

$$\left[O^{=}\right]_{ox} \longrightarrow \left[O\right]_{ox} + \left[O\right]_{met} + 2\ e^- \qquad (1c)$$

$$Zr + 2\left[O^{=}\right]_{ox} \longrightarrow 2\left[O_{\square}\right]_{ox} + ZrO_2 + 4\ e^- \qquad (1d)$$

where $\left[O^{=}\right]_{ox}$ = oxygen ion in the oxide lattice

$\left[O_{\square}\right]_{ox}$ = oxygen vacancy in the oxide lattice

$\left[O\right]_{met}$ = oxygen dissolved in the metal.

This oxidation region, ranging from an oxide-free surface to one bearing an approximately 200 Å thick layer, is characterized by the formation of a non-stoichiometric, anion deficient, oxide, the formation of a metal layer, adjacent to the oxide, enriched in dissolved oxygen and by a hundred percent uptake of hydrogen evolved by the corrosion reaction.
The oxidation rate in this region, being controlled by interface reactions, is nearly constant.
With increasing thickness of the oxide layer, above 200 Å, a gradual change in oxidation kinetics occurs. After the initial linear rate law a parabolic rate law is followed. Depending on alloy composition, in chemical and metallurgical sense, on corrosive medium and on temperature and pressure, this parabolic kinetics of the oxidation rate can further develop to a logarithmic function and finally a cubic rate law can be followed. For Zircaloy-2 corroding in high pressure, 300-400°C water and steam the transition from a linear to a cubic rate occurs in the oxide thickness region of 0.02-0.2 microns.
The cubic rate law is followed up to an oxide thickness of 2.3-2.5 microns. Considering the oxide as an electrolyte for cations, anions and electrons (F 1-4), at the boundaries of and in the oxide the following reactions are possible:

At the oxide-surface:

$$2H_2O + \left[Zr^{4+}\right]_{ox} \longrightarrow \left[Zr_{\square}\right]_{ox} + ZrO_2 + 4\,H^+ \qquad (2a)$$

$$4e^- + O_2 + \left[Zr^{4+}\right]_{ox} \longrightarrow \left[Zr_{\square}\right]_{ox} + ZrO_2 \qquad (2b)$$

$$H_2O + \left[O_{\square}\right]_{ox} \longrightarrow \left[O^{=}\right]_{ox} + 2\,H^+ \qquad (2c)$$

$$2e^- + H_2O + \left[O_{\square}\right]_{ox} \longrightarrow \left[O^{=}\right]_{ox} + 2\,H \qquad (2d)$$

$$4e^- + O_2 + \left[O_{\square}\right]_{ox} \longrightarrow \left[O^{=}\right]_{ox} + O^{=} \qquad (2e)$$

$$H^+ + e^- \longrightarrow H \qquad (2f)$$

$$H + H \longrightarrow H_2 \qquad (2g)$$

$$H + \left[O_{\square}\right]_{ox} \longrightarrow \left[H_o\right]_{ox} \qquad (2h)$$

In the oxide film:

$$\left[O^{=}\right]^1_{ox} + \left[O_{\square}\right]^2_{ox} \longrightarrow \left[O_{\square}\right]^1_{ox} + \left[O^{=}\right]^2_{ox} + O \qquad (3a)$$

$$\left[Zr_{\square}\right]^1_{ox} + \left[Zr^{4+}\right]^2_{ox} \longrightarrow \left[Zr^{4+}\right]^1_{ox} + \left[Zr_{\square}\right]^2_{ox} \qquad (3b)$$

$$\left[H_o\right]^1_{ox} + \left[O_{\square}\right]^2_{ox} \longrightarrow \left[O_{\square}\right]^1_{ox} + \left[H_o\right]^2_{ox} \qquad (3c)$$

The subscript 1 refers to a lattice place nearer to the oxide surface.

At the oxide-metal interface:

$$\left[O^{=}\right]_{ox} \longrightarrow \left[O_{\square}\right]_{ox} + \left[O\right]_{met} + 2e^- \qquad (4a)$$

$$\left[H_o\right]_{ox} \longrightarrow \left[O_{\square}\right]_{ox} + \left[H\right]_{met} \qquad (4b)$$

$$Zr + \left[Zr_{\square}\right]_{ox} \longrightarrow \left[Zr^{4+}\right]_{ox} + 4e^- \qquad (4c)$$

$$Zr + 2\left[O\right]_{met} \longrightarrow ZrO_2 \qquad (4d)$$

where $\left[Zr^{4+}\right]_{ox}$ = zirconium ion in the oxide lattice

$\left[Zr_{\square}\right]_{ox}$ = zirconium vacancy in the oxide lattice

$\left[H_o\right]_{ox}$ = hydrogen atom in an oxygen vacancy in the oxide lattice

$\left[O\right]_{met}$ = oxygen atom dissolved in the metal

$\left[H\right]_{met}$ = hydrogen atom dissolved in the metal.

According to this reaction scheme a p-type semi conducting oxide is formed at the oxide surface and a n-type oxide at the oxide metal interface. The growth of the oxide layer can be controlled by:

1. Boundary reactions 2a-2h
2. Migration of zirconium ions, electrons or oxygen ions in the oxide, according to reactions 3a-3c
3. Boundary reactions 4a-4d.

Davies and Dalgaard (F 5) showed that xenon atoms, embedded approximately 25 Å below the surface of Zircaloy-2, were still present at that depth below the oxide surface after corrosion in steam at 400-500°C. Therefore the reactions 2a, 2b, 3b and 4c can be neglected in oxidation rate kinetics considerations.
In view of the fact that Zirconium alloy, during pre-transition corrosion, corrode according to a parabolic, logarithmic or cubic rate law it is most likely that the oxidation rate kinetics is controlled by the migration of oxygen ions to the metal and the movement of electrons to the surface. Electrical neutrality for the oxide requires a current of electrons twice as large as the current of oxygen ions in the opposite direction. The concentrations and mobilities of the electrons and the oxygen ions, or better oxygen vacancies, are however not the same. Since the mobility of the electrons is much larger than that of the oxygen ions a potential field is formed over the oxide layer. The oxide film becomes negative at the oxide surface relative to the oxide-metal interface. The formation of this potential gradient is such that the current of electrons to the surface just matches the diffusion of oxygen ions to the metal. It must be noted that the electrons move against the potential field because their movement initially creates and then maintains the field. The initial difference in migration speed between electrons and oxygen ions disappears by slowing down of the electrons and speeding up of the oxygen ions. In view of this potential field it is not likely that hydrogen ions formed by the reaction 2c, penetrate and migrate in the oxide film.
Describing the oxidation process in terms of the well-known Wagner-Hauffe theory results in a parabolic oxidation rate law. For Zr-2.5% Nb and Zr-3% Nb-1% Sn this theory, or an adapted version of it gives a possible explanation of the oxidation process. Zircaloy-2 and Zircaloy-4 however corrode according to a cubic rate law in the pre-transition region.
Whether this cubic rate law, valid from 0.2-2.4 μ oxide thickness in water or steam at 300-400°C, is caused by electrical charges at the oxide surface and/or at the oxide-metal interface or by space charges in the boundary layers of the oxide film is as yet not known.
Because the Pilling-Bedworth ratio for the transformation $Zr \rightarrow ZrO_2$ is greater than unity, 1.55 for Zircaloy-2, stresses build up within the oxide film during its growth. After some time, which is dependent on alloy composition and temperature, these stresses are relieved by the formation of microcracks parallel to the surface. At this transition point the cubic or parabolic rate law oxidation mechanism transforms, more or less suddenly, to a linear rate law. The oxidation process is now controlled either by migration of oxygen ions through an oxide layer of constant thickness or by the reactions at the boundaries of the oxide film. For Zircaloy-2 the time to transition and the weight gains at transition as function of temperature are presented in table 4.
The hydridation rate is controlled by the reactions 2d, 2f, 2g and 2h and by the number of oxygen vacancies present at the oxide surface.
The diameter of an oxygen vacancy in the oxide lattice is about 2.6 Å. Interstitial sites between oxygen and zirconium ions in the oxide have diameters ranging from 0.2-1.13 Å at the oxide surface and from 0.1-0.6 Å in the bulk oxide. The hydrogen atom, having a diameter of 1.1 Å, enters the oxide therefore via an oxygen vacancy, see reaction 2h.
Movement of hydrogen atoms from the oxide surface towards the metal occurs, according to reaction 3c, by jumping from vacancy to vacancy.

The competition between reactions 2g and 2h results in a hydridation rate which can be expressed under constant conditions, as a percentage of the theoretical quantity of hydrogen evolved by reactions 2c and 2d. In the pre-transition region of the oxidation process this percentage is 33% for Zircaloy-2 and 10% for Zircaloy-4, Zr-2.5% Nb and Zr-3% Nb - 1% Sn. This difference can be attributed to Nickel, present in Zircaloy-2 and not in the other zirconium alloys. Apparently reaction 2g is hindered by the presence of NiO, or a mixed zirconium-nickel oxide, probably due to adsorption of atomic hydrogen on this oxide. The increase in hydridation percentage, after the transition to linear kinetics of Zircaloy-2 corroding in water or steam can be attributed to the adsorption of hydrogen atoms not only on the oxide-water surface but also in the overlying cracked oxide film. The percentage hydrogen uptake is not changed after transition for Zircaloy-4 and the Zr-Nb alloys. The lower hydridation rate in water containing oxygen can be attributed to a lower vacancy concentration at the oxide surface resulting in a decrease of reaction 2h. The higher hydridation rate in water containing large quantities of molecular hydrogen can be attributed to a decrease in reaction 2g, resulting in a higher concentration of atomic hydrogen, thus favouring reaction 2h.

The effect of irradiation on the oxidation and hydridation rate can be characterized in two general conclusions:

1. Acceleration of the corrosion process is observed if the specimens are exposed to steam under reactor conditions.
2. No effect on corrosion of Zirconium alloys is observed if the specimens are exposed to water under PWR conditions.

A simple but unsatisfactory explanation of these conclusions can be given if we attribute a possible irradiation effect to decomposition products of the water, or steam, formed by radiolysis. These decomposition products, radicals H, OH, HO_2 and molecules H_2 and H_2O_2, if available in sufficient quantities, can cause an increase in oxidation and hydridation rate. The concentrations of a decomposition product R is given by the relation (F 6):

$$R = (K_1^2 S^2 + K_2 G_R I)^{1/2} - K_1 S$$

where

G_R = reaction yield in number of species R formed by the absorption 100 ev. of energy in the solute
I = dose rate
S = concentration of the solute
R = concentration of the decomposition product R
K_1 and K_2 = constants.

Now under PWR conditions it is apparently so that $K_1^2 S^2 > K_2 G_R I$ resulting in a low valie of R. In steam atmosphere S is considerably lower so that than $K_2 G_R I < K_1^2 S^2$ resulting in a relatively high value of R.

G. Calculation of the safe life time of Zircaloy-2 canning in the NERO fuel element

1. Temperature and heat flow at the outer canning surface.

The inlet temperature of the cooling water in the NERO core is 285°C, the outlet temperature 315°C. Internal circulation of the water in the core and the temperature drop across the water-film adjacent to the canning surface make that the temperature at the oxide surface is considerably higher than the just mentioned 315°C.
The heat flow through the canning walls of the fuel rods in the NERO reactor has a maximum value of 126 W/cm^2 and a mean value of 35 W/cm^2. For life time calculations a heat flow of 100 W/cm^2 will be used because only very few of the thousands fuel rods present in the core are operating at a heat flow of 100-126 W/cm^2. At the operating pressure of 140 Kg/cm^2 and a waterflow of 0.21 Kg/cm^2 sec. this heat flow of 100 W/cm^2 makes that about 30% of the Zircaloy-2 canning surface, present in the NERO core, has a temperature of 345°C. Thus for the NERO fuel element life time calculations a heat flow of 100 W/cm^2 and an oxide-surface temperature of 345°C will be used.

2. Effect of heat flow through the canning wall

During operation in a reactor the heat transported through the canning causes a temperature gradient across the metal + oxide wall. Assuming that the temperature at the oxide surface remains constant during reactor operation, thus neglecting an eventually occuring crud deposition on the fuel rods, the growth of the zirconium-oxide film causes an increase in temperature at the oxide-metal interface. In part F of this report we have seen that it is not impossible that the temperature at the oxide-metal interface is the oxidation rate determining temperature. In taking this temperature as the rate controlling temperature we are not far from truth because cracking of the oxide film after transition makes that the mean temperature in the one micron thick oxide layer adhering to the metal is oxidation rate controlling. The temperature at the oxide-metal interface can be calculated with the formula:

$$T_i = T_s + \frac{q}{k} x \qquad (G.1)$$

where

T_i = temperature at interface
T_s = " " surface
x = oxide layer thickness in cm.
q = heat flow in cal/cm^2 sec.
k = heat conductivity, in cal/cm.sec. °C, of the oxide film.

In treating the oxide film as a flat surface instead of a cylindrical surface we make a negligible error. Now using the empirical relations presented in part D for Zircaloy-2 we derived the following relations:

$$t_{tr} = \left[5.55 \int_0^y \exp\left(\frac{5220}{T_i}\right) dx \right]^3 \qquad (G.2)$$

$$t_x = t_{tr} + 6.54 \cdot 10^{-5} \int_y^x \exp\left(\frac{14400}{T_i}\right) dx \qquad (G.3)$$

$$y = 8.20 \cdot 10^{-4} \exp\left(-\frac{790}{T_s}\right) = x_{tr} \qquad (G.4)$$

where

t_{tr} = time to transition, in days
y = oxide thickness at transition, in cm.
x = oxide thickness $t_x - t_{tr}$ days after transition, in cm.

The heat conductivity of oxide films, formed on Zirconium alloys in high temperature water, is 0.0033 cal/cm.sec. °C.
With the relations E.1-4 the time to reach a certain oxide thickness was calculated as a function of the oxide surface temperature and the heat flow.

3. Effect of irradiation on the oxidation rate

Although under constant PWR conditions no effect of irradiation is observed up till now, the number of investigators reporting an irradiation effect on the oxidation and hydridation rate is too large to neglect their results completely. Part of the effects found by these investigators can however be attributed to heat flow and thermal cycling effects. Therefore in our calculations an increase of the oxidation and hydridation rate by a factor 1.5 will be taken into account. The data calculated with the relations E.1-4 divided by a factor 1.5, are presented in table 6.

4. Absorption of hydrogen as a function of the oxide thickness.

The percentage of the hydrogen, liberated during the corrosion of Zircaloy-2 in high temperature water, that is absorbed in the canning wall is 33% in the pre-transition region and 75% in the post-transition region of the Zircaloy-2 oxidation curve. For Zircaloy-4, Zr-2.5% Nb and Zr-3% Nb - 1% Sn these percentages are 10% both in the pre- and in the post-transition region. In table 7 the mean hydrogen concentration, in ppm, absorbed in the canning wall is presented as a function of oxide film thickness, in μ, and canning wall thichness, in mm.

5. Distribution of hydrogen in the canning wall

The heat flow through the canning wall causes a difference in temperature between the inner and outer surface of the canning wall. This temperature gradient can be calculated with the relation:

$$T_i - t_o = \frac{r_o \cdot q}{k} \ln \frac{r_o}{r_i} \qquad (G.5)$$

where

T_i = temperature in °C at inner wall surface
T^i = " " " " outer " "
q^o = heat flow, in cal/cm^2.sec., at the outer wall surface
k = heat conductivity in cal/cm.sec. °C = 0.038 for Zircaloy-2 and 0.0033 for ZrO_2.
r_o = outer radius, in cm, of the canning tube = 0.595
r_i = inner " " " " " " " = 0.510

At the NERO heat flow of 23.9 cal/cm^2.sec., equivalent to 100 W/cm^2, we calculate a temperature difference between the oxide surface and the oxide-metal interface of 0.724°C/μ oxide thickness and a temperature difference of 57.7°C between the inner and outer surface of the metal wall. The temperature gradient is nearly constant throughout the metal wall. Under the influence of this temperature gradient dissolved hydrogen diffuses to the colder oxide-metal interface according to the relation:

$$J_x = - J_c - J_T = - D \frac{dc_x}{dx} - \frac{D\, c_x\, Q^*}{R\, T_x^2} \cdot \frac{dT_x}{dx} \qquad (G.6)$$

where

J_x = diffusion rate in ppm H cm^3/cm^2.sec. at x cm of the oxide-metal interface
J_c = diffusion rate caused by a concentration gradient
J_T = " " " " " temperature "
D = " coefficient of hydrogen in Zircaloy-2
c_x = hydrogen concentration in ppm, at place x
Q^* = heat of transport of hydrogen in Zircaloy-2 = 6000 cal/mole
R = gas constant per mole
T_x = temperature in °Kelvin at place x

The diffusion coefficient D can be calculated with the relation:

$$D = D_o \exp \left(- \frac{Q}{R\, T_x}\right) \qquad (G.7)$$

where

D_o = frequency factor = 2.17 . 10^{-3} cm^2/sec. for hydrogen in Zircaloy-2
Q = hydrogen diffusion activation energy of Zircaloy-2 = 8300 cal/mole

Because Q^* is positive hydrogen diffuses from warm to cold places in the Zircaloy-2 wall. Diffusion stops when $J_x = 0$ or $J_c = -J_T$. Integration leads then to the equilibrium condition.

$$c_x = K_H \exp \left(\frac{Q^*}{R\, T_x}\right) \qquad (G.8)$$

where

K_H = a constant for a given set of conditions.

If c_i and c_o are the hydrogen concentrations at the inner surface and the oxide-metal interface of the canning wall, the concentration c_i can be calculated with the relation, derived from G.8:

$$c_i = c_o \exp \left(- \frac{Q^*}{R} \cdot \frac{T_i - T_o}{T_i \cdot T_o}\right) \qquad (G.9)$$

The hydrogen concentration at the moment that the first hydrides are formed at the colder oxide-metal interface can be calculated with the relation:

$$(c_o)_{max} = c' \exp \left(- \frac{\Delta H}{R\, T_o}\right) \qquad (G.10)$$

where

$(c_o)_{max}$ = solid solubility of hydrogen, in ppm, in Zircaloy-2 at a temperature of T_o °Kelvin
c' = a constant = 8.50 . 10^4 ppm for Zircaloy-2
ΔH = heat of mixing = 7600 cal/mole for Zircaloy-2

For the fuel rod canning in the NERO core, operating at a heat flow of 100 W/cm^2 the calculated values of T_o, T_i, $(c_o)_{max}$, c_i and $\bar{c}_w$, the mean hydrogen concentration in the 0.085 cm thick wall, at the moment that the first hydrides precipitates, are presented in table 8 as a function of oxide thickness.
Combination of the calculated values presented in table 7 and 8 leads to the conclusion that at the time that an oxide thickness of 7.2 μ is reached the first hydrides are precipitated at the cold side of the 0.85 mm thick Zircaloy-2 canning wall operating at a heat flow of 100 W/cm^2 and having an oxide-surface temperature of 345°C. This moment is reached after 1.05 years reactor operation. Assuming that the solid solubility of hydrogen in Zircaloy-4 is equal to that in Zircaloy-2 it can be calculated that the first hydrides will precipitate in a 0.85 mm thick Zircaloy-4 wall at an oxide thickness of approximately 70 μ. The solid solubility of hydrogen in Zr-Nb is so high that the effect of hydrogen on the life time of canning tubes can be neglected.

6. Hydride layer thickness as a function of oxide thickness

With the data presented in table 7 and 8 the thickness of the hydride layer as a function of the oxide thickness can be calculated for Zircaloy-2 canning walls operating at a heat flow of 100 W/cm^2 and at an oxide-surface temperature of 345°C. For these calculations we have to use the following relations:

1. A 1 μ thick $ZrH_{1.6}$ layer equals a mean hydrogen concentration of 21 ppm in a 0.85 mm thick canning wall of Zircaloy-2
2. By the formation of a 1 μ thick ZrO_2 layer the metal wall thickness is decreased with 0.645 μ.
3. By the formation of a 1 μ thick $ZrH_{1.6}$ layer the metal wall thickness is decreased with 0.85 μ.

In table 9 are presented as a function of the oxide thickness:

H_t = total mean hydrogen concentration, including 20 ppm H_2 initially present
H_s = mean dissolved hydrogen concentration in the wall, in ppm
H_p = mean precipitated hydrogen concentration, in ppm
$+d_H$ = thickness of the hydride layer in μ
$+d_{H+O}$ = thickness of oxide + hydride layer in μ
$-d_{M_O}$ = decrease in metal wall thickness by the oxide layer, in μ
$-d_{M_{H+O}}$ = decrease in metal wall thickness by the oxide + hydride layer, in μ.

7. Critical hydride and oxide layer thickness

The Zirconium hydride platelets, precipitated during reactor operation at the colder, outer surface of the canning wall, can be oriented at ramdom or preferentially in the radial, or circumferential direction. Radially oriented hydrides increase the susceptibility to the formation of cracks perpendicular to the wall surface. These cracks can propagate within a short time to the inner wall surface causing failure of the fuel rod.
Therefore most manufacturers of Zircaloy-2 deliver their tubes in the recovery annealed condition, with a crystallographic texture which favours the circumferential orientation of precipitated hydrides. During reactor operation the platelets tend to precipitate perpendicularly to a tensile stress and to the heat

flow direction and parallel to a compressive stress. Assuming now that the fuel element construction is such that it favours circumferential orientation of the hydrides, the hydride limit is depending either on the thickness of the hydride layer or on the mean dissolved hydrogen concentration in the metal wall.
The dissolved hydrogen decreases the impact strength considerably. Under PWR conditions however the effect of irradiation on the impact strength dominates the hydrogen induced effect. At room temperature the impact strength of Zircaloy-2 irradiated to 10^{21} n/cm^2 is nearly the same for specimens containing 20, 100 and 250 ppm hydrogen.
From table 8 it can be seen that even at an oxide thickness of 40 μ the maximum dissolved hydrogen concentration in the metal wall is only 233 ppm. Zircaloy-2 cladding in the Shipping-port reactor, see table 3, has already been irradiated to 2.10^{22} n/cm^2 and is still operating satisfactory. It is therefore unlikely that dissolved hydrogen limits the use of Zircaloy-2 operating under PWR conditions. The tolerable increase in oxide film and hydride layer thickness is determined by the moment at which the layers scale off from the adjacent metal. Literature data of the scaling off point of Zirconium alloy canning tubes operating in high pressure, high temperature, circulating water are however scarce. The experimental results, obtained up till now in different countries, can be summarized in the following conclusions:

1. For isothermally tested Zircaloy specimens scaling off starts at an oxide thickness of approximately 35 μ
2. Zircaloy-2 canning tubes containing 500-800 ppm hydrogen failed during operation under PWR conditions
3. Up to a hydrogen content of 400 ppm Zircaloy canning can be used successfully.

A 500 ppm hydrogen content in our case corresponds, see table 9, with an oxide + hydride layer thickness of 35.9 μ. Therefore an oxide + hydride layer thickness of 35 μ will be used as the canning life time limiting factor.
For Zircaloy-4 and the Zr-Nb canning tubes, in which no hydrides are precipitated at an oxide thickness of 35 μ, a canning life time limiting oxide thickness of 35 μ will be used. This oxide resp. oxide + hydride layer thickness of 35 μ corresponds, see table 9, to a decrease in metal wall thickness of 22.6 and 25.7 μ respectively.
For fully and recovery annealed Zircaloy-2 this decrease in wall thickness corresponds to the consumption of a 1-2 grain thick surface layer. Thus it is apparently so that the scaling off process starts when grains adjacent to a corrosion consumed grain, which is completely transformed in oxide or oxide + hydride, can be expelled easily from the surface by the flowing water.

8. Safe life time expectancy of Zirconium alloy canning tubes operating under NERO conditions

Before drawing the final conclusion of this report it is useful to recapitulate all more or less discussible assumptions on which the calculations and conclusions are based.

1. In 300-600°C water the oxidation rate of Zircaloy-2 and Zircaloy-4 is given by the relations:

$$W_{pre} = 27.1 \cdot 10^{3} \cdot t^{1/3} \cdot \exp\left(-\frac{5220}{T}\right)$$

$$W_{post} = 23.0 \cdot 10^{8} \cdot t \cdot \exp\left(-\frac{14400}{T}\right)$$

2. The oxidation rate of Zr-Nb-alloys is a factor two higher than that of the Zircaloys in the pre-transition region of the oxidation curve. Beyond transition these alloys behave very similarly.
3. Under PWR conditions the oxidation rate is increased by a factor 1.5.
4. The percentage of hydrogen pick-up is 33% and 75% for Zircaloy-2 in respectively the pre- and post-transition region of the oxidation process.
5. For Zircaloy-4 and the Zr-Nb-alloy the hydrogen pick-up percentage is 10% as well in the pre- as in the post-transition region.
6. The oxidation rate is controlled by the temperature at the metal-oxide interface.
7. Zirconium alloy tube fabrication history and fuel element construction favour the circumferential orientation of precipitated hydrides in the canning wall.
8. The fuel element construction is such that fretting corrosion, for example at spacer locations, does not occur or at least does not impair the canning life time.
9. The maximum tolerable oxide or oxide + hydride layer thickness, on Zirconium alloy canning tubes, is 35 μ.
10. The decisive NERO conditions for canning life time calculations are a heat flow of 100 W/cm^2 and a temperature of 345°C at the oxide-surface.

Furthermore it must be noted that the calculations take account of the increase in oxidation rate under the influence of the heat flow and of the distribution in the metal wall of absorbed hydrogen in the radial but not in the axial direction.

In figure 1 the oxide + hydride thickness of Zircaloy-2 and the oxide thickness of Zircaloy-4 and the Zr-Nb-alloys are presented as a function of time of the NERO canning operating under PWR conditions at a heat flow of 100 W/cm^2 and an oxide-surface temperature of 345°C.
The curves lead to the conclusion that the expectable safe life time of Zirconium alloy canning tubes operating under NERO conditions is 2.40 years for Zircaloy-2, 3.40 years for the Zr-Nb-alloys and 3.60 years for Zircaloy-4.

9. Discussions of the calculated life time data

The life time data, presented in the conclusions above indicate that the continuous use of Zirconium alloys as canning material during 3.3 years in the NERO reactor operating at full power is hardly attainable. The use of Zircaloy-2 must even be dissuaded. In view of the many more or less uncertain assumptions which had to be used in the calculations the mentioned life time data need however experimental confirmation before a certain Zirconium alloy can be excluded as canning material for the NERO fuel rods. Apart from the effect of heat flow on hydrogen distribution in the wall but assuming a 1.5 times increase in oxidation rate caused by the

radiation field in a reactor the test temperature in isothermally performed tests in out-of-pile loops or autoclaves must be 370-380°C in order that the test results are, from a corrosion point of view, comparable with tests performed under NERO conditions. Because the critical temperature of water is 374°C loops designed and constructed for the circulation of high pressure water are not suitable for tests at 370°-380°C. Therefore superheat or supercritical steam loops have to be used for these experiments.

The life time calculations presented in this report were based on the assumption that corrosion limits this time. But the gradual change in mechanical properties during reactor operation, as for example the decrease in ductility and increase in creep rate, must also be considered as possible life time limiting factors. Zircaloy-2 clad fuel rods were tested in a pressurized water loop in the Canadian NRX reactor for 18 months at a canning surface temperature of 260-280°C and a heat flow of 45-75 W/cm^2. Although an approximately 30% increase in room temperature U.T.S. was accompanied by a fourfold decrease in ductility, at a maximum hydrogen concentration of 100 ppm in the cladding wall, the tested fuel rods did not show cladding failures. The Zircaloy-2 clad blanket fuel rods in Shipping-port Core 1 operated without important failures during almost 3 years at a cladding surface temperature of 268°C, an average heat flow of 49 W/cm^2 and a maximum heat flow of 130 W/cm^2. Moreover it is known that recovery rates of radiation damage in Zircaloy-2 increase with increasing irradiation temperature. The cladding wall temperatures in the NERO reactor is 80°C higher than those in the cladding wall of the Shipping port blanket fuel rods. It is therefore quite possible, and can even be expected, that the decrease in mechanical integrity caused by the radiation field is not a life time limiting factor for the Zirconium alloy cladding wall in the NERO reactor.
The increase in crack propagation susceptibility, caused by hydrogen and oxygen absorbed in the wall during reactor operation, is most likely the cladding life time limiting factor. Especially during reactor shut down periods, when for example a nuclear ship is towed into a harbour by a tug, this susceptibility to crack propagation can cause fuel rod failures.

Summary

Based on the present day knowledge of the oxidation and hydridation behaviour of Zirconium alloys under PWR conditions a calculation of the safe life time expectancy of Zirconium alloy canning in the fuel elements of the NERO reactor is presented. The decisive NERO conditions for life time calculations are a heat flow of 100 W/cm^2 and a temperature of 345°C at the oxide-water surface.
The calculations take account of the increase in oxidation rate under the influence of the heat flow and of the distribution of absorbed hydrogen in the canning wall in the radial direction.
The maximum tolerable oxide or oxide + hydride layer thickness, on Zirconium alloy canning tubes was fixed at 35 µ.
The calculated data led to the conclusion that from the corrosion point of view the safe life time of Zirconium alloy canning tubes, having a wall thickness of 0.85 mm, operating under NERO conditions is 2.40 years for Zircaloy-2, 3.40 years for Zr-2.5% Nb and Zr-3% Nb-1% Sn, and 3.60 years for Zircaloy-4.

References

A. Physical factors

1. HW-82651, July 1964, V.H. Troutner a.o., p. 5.17
2. HW-80021, March 1964, W.K. Winegardner
3. WAPD-MRP-110, November 1964, J. Hino, p. 56
4. see A.1, D.W. Shannon, p. 5.15
5. GEAP-4089, November 1962, Vol. II, B. Cox, p. 16-1/16-20
6. F.H. Krenz, First Int.Congr.Metal Corrosion, London 1961, p.462-471, Butterworths
7. J.H. Dyce, Nuclear Engineering, July 1964, p. 253-255

B. Chemical factors

1. see A.3, J. Hino, p. 62 and 65
2. see A.3, J. Hino, p. 53 and 55
3. WAPD-TM-411, November 1964, E. Hillner, p. 4-6
4. HW-72266, 1962, H.P. Maffei
5. W.E. Berry a.o., Corrosion 17 (1961), p. 109-117
6. WAPD-MM-184, February 1953, K.M. Goldman, D.E. Thomas
7. WAPD-BT-24, December 1961, S. Kass, W.W. Kirk
8. B. Lustman a.o., Nucleonics 19 (1961), p. 58-63
9. see B.3, p. 14
10. see A.3, p. 62
11. WAPD-TM-307, August 1962, E. Hillner, J.N. Chirigos
12. see B.3, p. 19-22

C. Irradiation effect

1. HW-76636, 1962, W.A. Burns, H.P. Maffei
2. Geneva conference, 1964, paper 21, W.R. Thomas a.o.
3. see A-5, R.C. Nelson, p. 17.1-17.29
4. HW-82651, July 1964, H.P. Maffei, p. 5.13-14
5. see C.4, W.A. Burns, p.5.1-5.3
6. AERE-R-4820, December 1964, J.K. Dawson
7. W. Yeniscavich, J. Nuclear Materials 1 (1959), p. 271-280
8. WAPD-TM-264, February 1961, B. Rubin, p. 18
9. WAPD-TM-308, December 1961, L.R. Lynam, p.7
   WAPD-TM-326, April 1963, L.R. Lynam, p.12
9. HW-67949 Rev., December 1962, L.J. Defferding, p.3
10. S.B. Dalgaard, Corrosion or reactor materials, IAEA conference proc., Vienna 1962, Vol.II, p.175
11. WAPD-TM-433, August 1964, L.R. Lynam
12. AERE-R-4779, November 1964, P.J. Harrop a.o.

F. Oxidation and hydridation mechanism

1. see B.3, E. Hillner, p. 31-35
2. D.L. Douglas, see C.10, p. 225-255
3. W.D. Kingery, Kinetics of high temperature processes, 1958, p. 37-44 John Wiley N.Y.
4. K. Hauffe, see F.3, p. 282-293
5. AECL-2066, September 1964, S.B. Dalgaard
6. A.O. Allen, Radiation chemistry of water and aqueous solutions, 1961, v. Nostrand, N.Y.

G. Life time calculations

1. AECL-919, September 1959, G.J. Biefer a.o.
2. AECL-1411, October 1961, A. Sawatzky, E. Vogt
3. AECL-1626, October 1962, F.H. Krenz
4. see A.7
5. WAPD-TM-104, January 1958, J.M. Markowitz
6. ORNL-3281, July 1962, C.L. Whitmarsh

Table 1.

Oxidation and Hydridation of α-annealed Zircaloy-2 in water at 360°C

	Test time in days								
Degassed water	3	10	50	100	150	200	300	400	500
Weight gain in mg/dm^2	11	14	23	28.5	33	52	82	112	142
Hydrogen " " "	0.30	0.49	1.04	1.31	1.59	2.60	5.3	8.1	10.8
Total hydrogen pick-up percentage	22	28	36	37	38	40	52	58	61
Degassed water + 70 atm oxygen									
Weight gain in mg/dm^2	15	18	27	36	52	73	115	154	220
Hydrogen " " "	0.18	0.20	0.21	0.23	0.33	0.46	0.72	0.96	1.38
Total hydrogen pick-up percentage	10	9	6	5	5	5	5	5	5
Replenished degassed water									
Weight gain in mg/dm^2	12	17	23	30	34	42	70	97	124
Hydrogen " " "	0.44	0.72	0.94	1.19	1.45	2.3	4.2	-	-
Total hydrogen pick-up percentage	29	34	34	32	34	44	48	-	-

Table 2

Corrosion and Hydrogen absorption of Zircaloy in 322°C oxygen free, pH = 10 recirculating water.

Material	Hydrogen	Measured value	Test time in days									Cumulative ΔH % in pre-transition region
			30	60	116	174	233	293	410	533	652	
Zircaloy-2 α-annealed	0.03 cm^3/kg	ΔW mg/dm^2	15	17	21	22	24	25	28	30	35	
		ΔH mg/m^2	18	36	43	36	43	43	41	76	97	24
		ΔH %	10	18	17	13	15	14	12	20	22	
	55 cm^3/kg	ΔW mg/dm^2	16	18	22	24	27	28	31	42	57	
		ΔH mg/m^2	38	44	55	69	67	68	80	157	252	30
		ΔH %	19	18	20	23	20	19	21	30	34	
Zircaloy-2 β-treated	0.03 cm^3/kg	ΔW mg/dm^2	14	16	20	25	25	26	29	33	43	
		ΔH mg/m^2	37	45	54	68	69	59	62	63	135	20
		ΔH %	21	21	24	23	24	20	17	15	24	
	55 cm^3/kg	ΔW mg/dm^2	16	19	23	26	28	30	37	50	63	
		ΔH mg/m^2	60	76	123	145	132	146	193	214	401	40
		ΔH %	29	34	43	46	38	43	42	37	52	
Zircaloy-4 α-annealed	0.03 cm^3/kg	ΔW mg/dm^2	14	16	19	21	22	25	27	29	36	
		ΔH mg/m^2	16	28	15	17	18	25	27	26	40	9
		ΔH %	9	10	7	7	6	8	7	7	9	
	55 cm^3/kg	ΔW mg/dm^2	14	17	19	22	24	26	30	43	54	
		ΔH mg/m^2	34	25	25	27	37	38	42	61	108	11
		ΔH %	20	12	11	10	12	11	11	11	16	
Zircaloy-4 β-treated	0.03 cm^3/kg	ΔW mg/dm^2	13	14	18		22	23	28	31	39	
		ΔH mg/m^2	20	19	17		30	30	34	35	37	8
		ΔH %	13	11	8		11	11	11	9	8	
	55	ΔW mg/dm^2	13	16	19		24	28	32	42	56	
		ΔH mg/m^2	33	22	31		38	-	-	50	76	10
		ΔH %	20	11	13		13	-	-	10	11	

Table 3

Zircaloy-2 cladding behaviour in Shipping-port PWR, calculated and measured values.

	Before conditioning	Before Seed 1	After Seed 1	After Seed 2	After Seed 3
Total exposure time in days	-	3	660	1122	1519
Total exposure time EFPH	-	-	5800	13700	21000
Average heat flux W/cm^2	-	-	48.2	48.2	48.8
Integrated fast flux nvt x 10^{-21}	-	-	5.8	13.0	20.0
Av. UO_2 burn-up $Fiss/cm^3$ x 10^{-20}	-	-	1.9	3.8	6.4
Av. clad surface temp. ^oC	-	360	265	268	268
Calculated incremental increase:					
in oxide thickness μ	-	0.60	0.60	0.30	0.13
in hydrogen content ppm	40	9	9	4	2
calculated total:					
oxide thickness in μ	-	0.60	1.20	1.50	1.63
hydrogen content in ppm	40	49	58	62	64
Measured:					
oxide thickness in μ					1.17-2.54
hydrogen content in ppm				47±9	57±7

Table 4

Oxidation constants for α-annealed Zircaloy-2.

Temperature in °C	300	320	340	360	400
K_c, cubic rate constant	3.00	4.08	5.43	7.12	11.6
K_l, linear rate constant	.0281	.0656	.145	.303	1.17
t_{tr}, time to transition in days	1118	513	247	125	36
W_{tr}, weight gain at transition mg/dm^2	31.0	32.5	33.9	35.3	38.0

Table 5

Some fundamental data of Zircaloy-2 and Zirconium dioxide

Zircaloy-2		
Density in gram/cm^3	6.57	
Atoms Zr/cm^3	44.4	10^{21}
" Zr/cm^2	12.35	10^{12}
Solubility of Oxygen at 300-400°C		
weight %	6.50	
atoms O/cm^3	15.67	10^{21}
" O/cm^2	6.26	10^{14}
1000 ppm Oxygen equals		
weight %	0.1	
atoms O/cm^3	0.24	10^{21}
" O/cm^2	0.385	10^{14}
Zirconium dioxide		
Density in gram/cm^3	5.73	
atoms O/cm^3	56.	10^{21}
" O/cm^2	14.6	10^{14}
Solubility of Zirconium		
weight %	0.83	
atoms Zr/cm^3	0.31	10^{21}
" Zr/cm^2	0.46	10^{14}

A weight gain of 15 mg/dm^2 ≡ + 1.008 μ ZrO_2 ≡ - 0.651 μ Zr metal

An oxidation rate of 1 mg/dm^2.day equals a reaction rate of $4.35.10^{12}$ atoms O/cm^2.sec.

Diffusion coefficient in cm^2/sec. of Oxygen

Temperature °C	D zircaloy-2 x 10^{18}	D zirconium oxide x 10^{14}
300	0.22	1.27
320	0.99	3.12
340	4.25	8.46
360	16.2	18.8
400	179.	93.2

Table 6

Reactor operating time, in years, for Zircaloy-2 canning tubes operating under PWR conditions as a function of oxide film thickness, in μ, heat flow and temperature at the oxide surface.

Temperature °C at oxide surface	Heat flow in W/cm²	Time in years to reach an oxide thickness in μ of: x_{tr}*	4	6	8	12	16	20	30	40
280	0	4.67	9.55	14.4	19.2	28.8	>30	>30	>30	>30
	63	4.63	9.24	13.6	17.8	25.7	>30	>30	>30	>30
	126	4.52	8.85	12.8	16.4	22.8	28.2	>30	>30	>30
	189	4.40	8.50	12.0	15.2	20.4	24.5	27.7	>30	>30
	252	4.30	8.15	11.3	14.1	18.3	21.4	23.7	27.2	28.9
300	0	2.04	3.90	5.82	7.74	11.6	15.4	19.3	28.9	38.5
	63	2.00	3.78	5.55	7.27	10.5	13.5	16.2	22.2	27.2
	126	1.95	3.63	5.24	6.73	9.38	11.7	13.6	17.4	20.0
	189	1.90	3.49	4.95	6.25	8.44	10.2	11.6	14.0	15.5
	252	1.86	3.36	4.68	5.82	7.63	8.99	10.0	11.6	12.4
320	0	0.94	1.69	2.51	3.33	4.96	6.60	8.23	12.3	16.4
	63	0.91	1.64	2.41	3.14	4.54	5.85	7.05	9.72	11.9
	126	0.89	1.58	2.28	2.93	4.09	5.11	5.98	7.71	8.93
	189	0.87	1.52	2.16	2.73	3.71	4.49	5.14	6.27	6.97
	252	0.85	1.47	2.05	2.56	3.37	3.99	4.47	5.23	5.63
340	0	0.45	0.78	1.15	1.53	2.28	3.03	3.78	5.66	7.53
	63	0.44	0.75	1.10	1.44	2.08	2.68	3.23	4.47	5.53
	126	0.43	0.73	1.05	1.34	1.88	2.36	2.77	3.60	4.20
	189	0.42	0.70	1.00	1.26	1.72	2.09	2.40	2.96	3.31
	252	0.41	0.68	0.95	1.19	1.58	1.87	2.11	2.49	2.70
360	0	0.23	0.37	0.55	0.73	1.08	1.44	1.79	2.67	3.56
	63	0.22	0.36	0.53	0.69	1.00	1.29	1.56	2.17	2.69
	126	0.22	0.35	0.51	0.65	0.91	1.14	1.35	1.76	2.07
	189	0.21	0.34	0.48	0.61	0.83	1.02	1.18	1.46	1.65
	252	0.21	0.33	0.46	0.58	0.77	0.92	1.04	1.24	1.36
NERO conditions:										
	0	0.37	0.65	0.95	1.26	1.88	2.51	3.08	4.65	6.12
345	100	0.36	0.62	0.88	1.14	1.63	2.07	2.45	3.24	3.90
	126	0.35	0.60	0.86	1.12	1.57	1.97	2.32	2.98	3.50

*) x_{tr} = oxide thickness at transition point in the oxidation curve:
= 1.97, 2.07, 2.17, 2.26, 2.28 and 2.35 μ at respectively 280, 300, 320, 340, 345 and 360°C.

Table 7

Hydrogen concentration, in ppm, absorbed in Zirconium alloy canning walls as a function of the oxide thickness, in μ, and wall thickness, in mm.

Oxide film thickness in μ		x_{tr}^{*}	4	6	8	12	16	20	30	40
Wall thickness in mm	Zirconium-alloy									
0.55	Zircaloy-2	40	105	184	264	423	582	741	1081	1421
0.70	"	31	83	145	207	331	456	580	891	1203
0.85	"	26	68	119	171	274	377	480	737	994
1.00	"	22	58	101	145	232	319	406	624	842
0.55	Zr-4/ZrNb/ZrNbSn	12	21	31	42	63	84	105	158	221
0.70		10	17	25	33	50	66	83	124	166
0.85		8	14	20	27	41	55	69	103	137
1.00		7	12	17	23	35	46	58	87	116

x_{tr}^{*} = oxide thickness at transition point, see souscript table 6.

Zirconium alloy tubes, delivered by European manufacturers, contain 10-30 ppm hydrogen. The total concentration of hydrogen in the canning walls is therefore 10-30 ppm higher than the value presented in table 7 for a given oxide thickness.

Table 8

Hydrogen concentrations, in ppm, in the Zircaloy-2 canning walls of NERO fuel rods, at the moment that the first hydride will precipitate in the wall.

Oxide thickness in μ	4	6	8	12	16	20	30	40
t_o, oxide-metal temp. °C	348	349	351	354	357	359	367	374
t_i, inner wall temp. °C	406	407	409	412	415	417	425	432
$(c_o)_{max}$, in ppm H	181	183	187	193	199	203	218	233
c_i, in ppm H	120	123	125	129	133	137	148	160
$\bar{c}_w$, in ppm H	148	150	153	158	162	166	178	191

Table 9

Hydrogen concentrations, hydride layer thickness and wall thickness decrease for Zircaloy-2, 0.85 mm thick, canning walls, operating at a heat flow of 100 W/cm^2 and externally cooled with 335°C water, as a function of oxide layer thickness.

Oxide thickness in μ	4	6	8	12	16	20	30	40
H_t, in ppm	88	139	191	294	397	500	757	1014
H_s, in ppm	88	139	153	158	162	166	178	191
H_p, in ppm	0	0	38	136	235	335	579	823
$+d_H$, in μ	0	0	1.8	6.5	11.2	15.9	27.6	39.2
$+d_{H+O}$, in μ	4	6	9.8	18.5	27.2	35.9	57.6	79.2
$-d_{M_O}$, in μ	2.6	3.9	5.2	7.7	10.3	12.9	19.4	25.8
$-d_{M_{H+O}}$, in μ	2.6	3.9	6.7	13.3	19.9	26.5	42.9	59.2

Figure_1

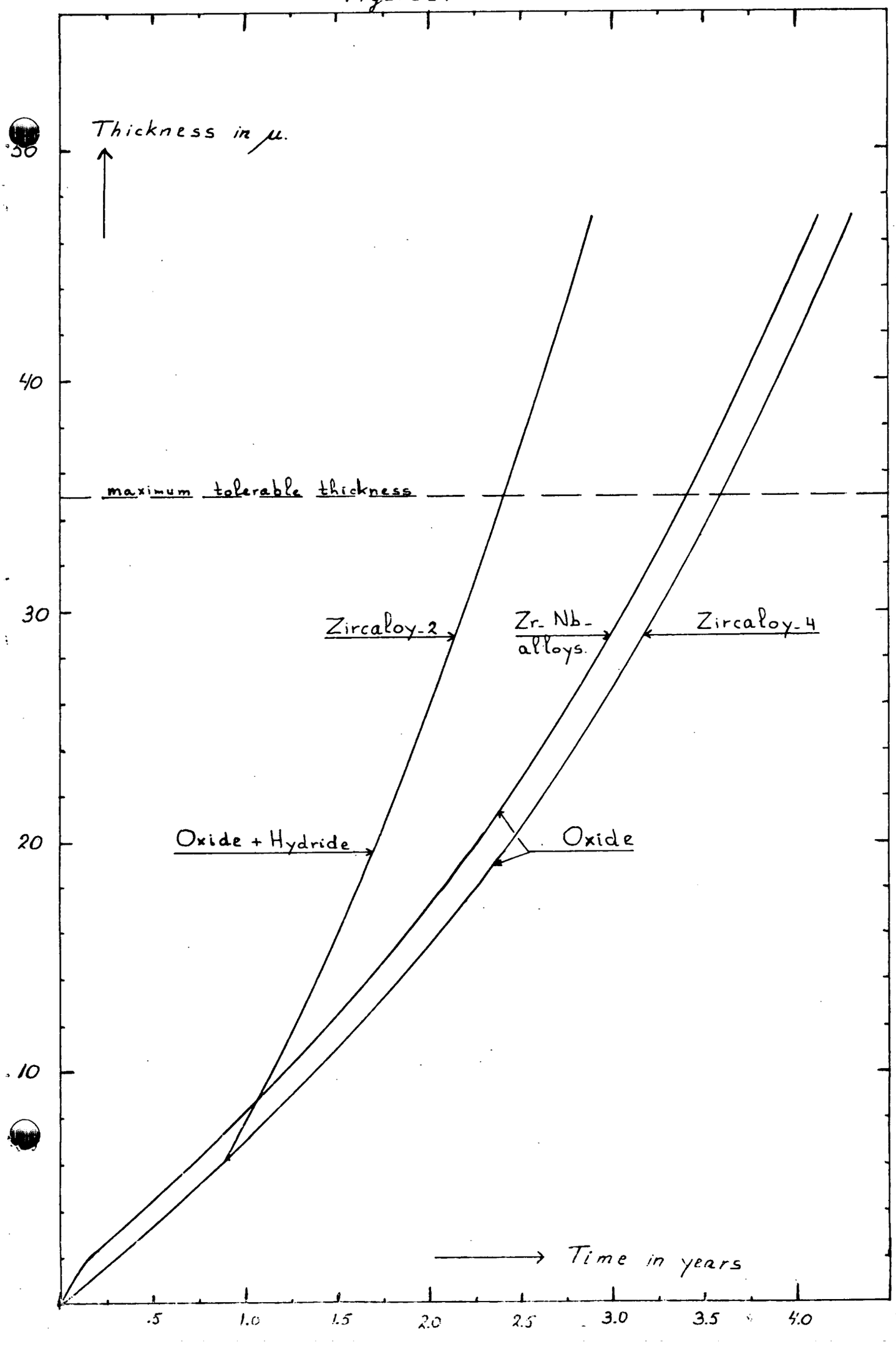
Thickness in μ.
50
40
30
20
10
maximum tolerable thickness
Zircaloy-2
Zr-Nb-alloys.
Zircaloy-4
Oxide + Hydride
Oxide
Time in years
.5
1.0
1.5
2.0
2.5
3.0
3.5
4.0